Electronic Supplementary Material (ESI) for Journal of Materials Chemistry C

Electronic Supplementary Information

Correlation between native defects and dopants in colloidal lanthanide-doped Ga_2O_3 nanocrystals: A path to enhancing functionality and controlling optical properties

Ting Wang, Arunasish Layek, Ian D. Hosein, Vadim Chirmanov and Pavle V. Radovanovic*

Department of Chemistry, University of Waterloo, 200 University Avenue West, Waterloo, Ontario N2L 3G1, Canada

* To whom correspondence should be addressed. E-mail: pavler@uwaterloo.ca

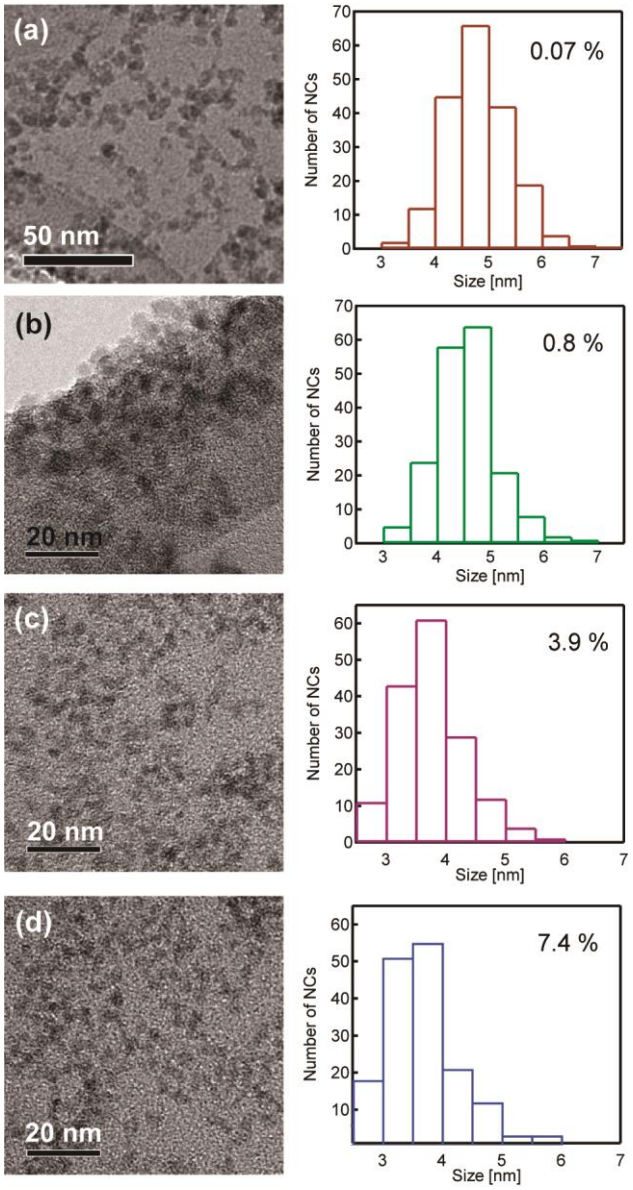

Fig. S1 TEM images (left) and size distribution histograms (right) of Eu^{3+}-doped Ga_2O_3 NCs with an average Eu^{3+} doping concentration of: (a) 0.07%, (b) 0.8%, (c) 3.9%, and (d) 7.4%.

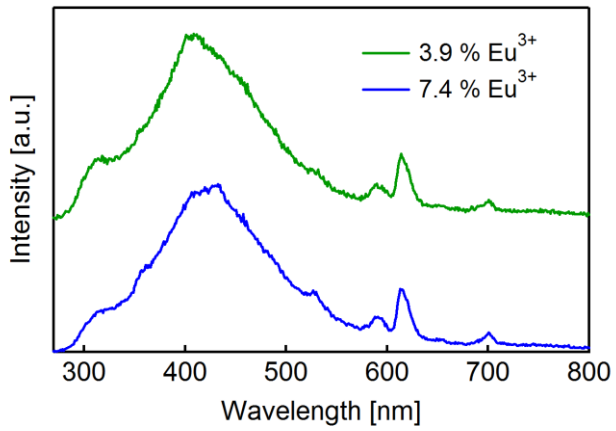

Fig. S2 Steady-state PL spectra of highly Eu^{3+}-doped (3.9 and 7.4 % doping concentrations) Ga_2O_3 NCs. Eu^{3+} intra-4f transitions are readily observed even in steady-state spectra.

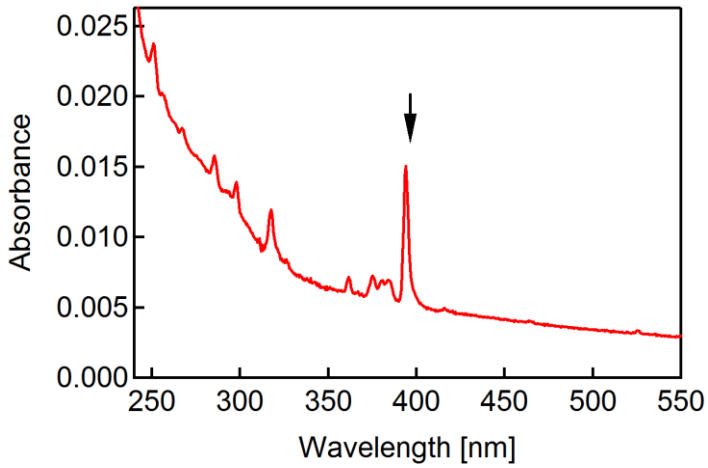

Fig. S3 Typical electronic absorption spectrum of Eu^{3+} in an aqueous solution. The arrow indicates $^7F_0 \rightarrow {}^5L_6$ transition used for direct excitation of Eu^{3+}.

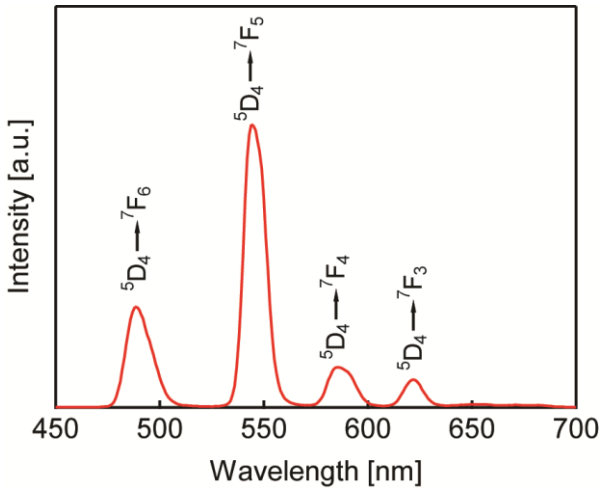

Fig. S4 Time-gated PL spectrum of 10 % Tb^{3+}-doped Ga_2O_3 NCs, showing the assignment of the observed f-f transitions.

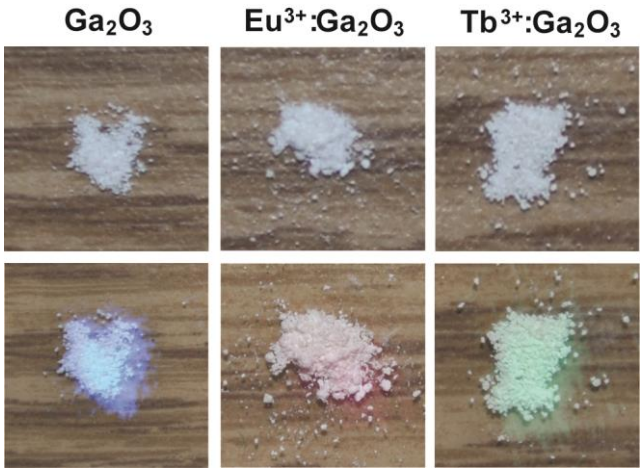

Fig. S5 Photographs of γ-Ga_2O_3 (left), 7.4 % Eu^{3+}-doped Ga_2O_3 (middle), and 10 % Tb^{3+}-doped Ga_2O_3 NC powders (right). Top and bottom panels compare the day-light photographs of isolated samples (top), and the same samples illuminated with 250 nm UV light (bottom). The luminescence can be clearly observed even in day light.

Table S1. Half-life of the DAP emission of Eu^{3+}-doped γ-Ga_2O_3 NCs for different doping concentrations.

Eu^{3+} doping conc. (%)	half-life (μs)
0	5.67
0.04	5.18
0.07	4.70
0.2	4.55
0.5	4.05

Table S2. CIE color coordinates (*x*, *y*) of 0.07 % Eu^{3+}-doped γ-Ga_2O_3 NCs for varying delay times calculated from the PL spectra in Fig. 8a.

delay time (ms)	*x*	*y*
0 (steady-state)	0.210	0.268
0.1	0.274	0.335
0.3	0.338	0.337
0.5	0.385	0.341
0.7	0.414	0.345
1.1	0.451	0.349
1.7	0.475	0.352